Quantum Criticality at the Superconductor-Insulator Transition Probed by the Nernst Effect

A. Roy, E. Shimshoni, and A. Frydman
Department of Physics, Bar Ilan University, Ramat Gan 52900, Israel

(Received 26 January 2018; published 27 July 2018)

The superconductor-insulator transition (SIT) is an excellent example of a quantum phase transition at zero temperature, dominated by quantum fluctuations. These are expected to be very prominent close to the quantum critical point. So far, most of the experimental studies of the SIT have concentrated on transport properties and tunneling experiments that provide indirect information on criticality close to the transition. Here we present an experiment uniquely designed to study the evolution of quantum fluctuations through the quantum critical point. We utilize the Nernst effect, which has been shown to be effective in probing superconducting fluctuation. We measure the Nernst coefficient in amorphous indium oxide films tuned through the SIT and find a large signal on both the superconducting and the insulating sides, which peaks close to the critical point. The transverse Peltier coefficient α_{xy}, which is the thermodynamic quantity extracted from these measurements, follows quantum critical scaling with critical exponents $\nu \sim 0.7$ and $z \sim 1$. These exponents are consistent with a clean X–Y model in $2+1$ dimensions.

DOI: 10.1103/PhysRevLett.121.047003

Quantum fluctuations are crucial for understanding fundamental physics from the atomic scale to the scale of the Universe. Most prominently, they are the driving force behind a quantum phase transition (QPT) between two competing phases of matter at zero temperature [1]. An experimentally versatile example for a QPT is the superconductor-insulator transition (SIT) in thin superconducting films, which is driven by quantum fluctuations and controlled by a nonthermal tuning parameter g. For $g < g_c$, the film is a superconductor, and for $g > g_c$, the system becomes insulating. Experimentally, different g's have been used to drive the transition, including inverse thickness [2–13], magnetic field [7,8,14–24], disorder [22,25–27], chemical composition [28], and gate voltage [29–31]. Though the quantum critical point ($g = g_c$) occurs at zero temperature, it also profoundly affects the behavior of the system at finite temperature. In the quantum critical regime, the system is neither superconducting nor insulating and is dominated by quantum fluctuations. These fluctuations of the superconducting order parameter $\psi = \psi_0 e^{i\theta}$ can be both amplitude (ψ_0) and phase (θ) fluctuations, which are interrelated via the uncertainty principle.

While much progress has been made in the field over the years, both theoretically and experimentally, there are still important open questions concerning phenomena close to the SIT. In particular, to this date, it remains controversial which universality class best describes the observed transitions and to what extent it varies between different specific realizations. From a theoretical point of view, a prototypical model that captures quantum fluctuations in ψ can be cast in terms of repulsively interacting bosons such as the Bose-Hubbard model, or equivalently, an array of Josephson-coupled superconducting islands where a charging energy E_C competes with the Josephson energy E_J [32–34]. This introduces a natural tuning parameter, e.g., $g = E_C/E_J$. However, a generic model of relevance to the physical system involves additional parameters that may profoundly affect the SIT: a chemical potential (which tunes the occupation of bosons per site), a magnetic field, and disorder, introduced as randomness in all the above parameters. This suggests a variety of quantum critical points with distinct critical behavior, manifested by different possible values of the critical exponents characterizing, e.g., the divergence of the correlation length ξ and time ξ_τ with the deviation from the quantum critical point $\Delta g = g - g_c$ [1]

$$\xi \sim |\Delta g|^{-\nu}, \qquad \xi_\tau \sim \xi^z. \tag{1}$$

In the clean limit, the insulating phase is interaction dominated (a Mott insulator). The dynamical critical exponent z depends on the commensurability of boson occupations and is either $z = 1$, if particle-hole symmetry is obeyed, or $z = 2$ at generic filling. In the former case, the SIT can be mapped to the classical 3D X–Y model, yielding $\nu \approx 2/3$ [35,36]. Disorder introduces an intermediate, gapless insulating phase dubbed "Bose glass" [33], which undergoes a direct transition to a superfluid. The critical exponents were argued to be $z = d$ (i.e., $z = 2$ in 2D) and $\nu \geq 1$, whereas long-range Coulomb interactions imply $z = 1$ [37]. Extensive numerical works over the past two decades [38–42], addressing arbitrarily large disorder strength and the role of magnetic field, have yielded estimates of $1 < z < 2$ (e.g., $z = 1.52$ in [42]) and various values of ν consistent with the bound $\nu \geq 1$.

On the experimental front, so far, attempts to provide the critical exponents were based on dc transport via scaling analyses of resistivity data [15,30,31,43–52]. Typically, these experimental results are consistent with $z = 1$, but the reported values of ν range from 0.4 to 2.3 and do not obviously agree with the theoretical predictions. Indeed, resistivity is possibly not an ideal probe of critical fluctuations in the order parameter field, since it is sensitive to details such as the specific scattering mechanism, inhomogeneities, etc. Moreover, it is not a thermodynamic quantity and is inherently nonequilibrium. Quantum fluctuations close to the SIT have been observed in thermodynamic measurements, e.g., of specific heat [13] and susceptibility [28]. However, these have not provided quantitative information on the critical behavior.

A promising candidate for fluctuation studies is the Nernst effect, i.e., the appearance of a transverse electric field in the presence of a longitudinal thermal gradient and a perpendicular magnetic field [53–59]. In recent years, a substantial Nernst signal $N = E_y/(-\nabla_x T)$ was measured around and above the critical temperature T_c in the underdoped regime of high-T_c superconductors [60] and in 2D disordered (NbSi and InO_x) films [61,62]. In the latter, it was shown that the unexpectedly large Nernst effect is due to the motion of vortices above the Berezinskii-Kosterlitz-Thouless temperature T_{BKT}. However, up to date, there has been no experimental study of the Nernst effect throughout the entire SIT.

Recent theoretical studies on quasi-1D Josephson junction arrays predict a pronounced peak of N close to the SIT due to quantum phase fluctuations [63,64]. This peak grows as the temperature is lowered towards $T = 0$. A qualitatively similar behavior was predicted to hold for a 2D system as well.

In this Letter, we describe a comprehensive measurement of the Nernst effect on an amorphous indium oxide (InO_x) film driven continuously through a disorder-induced SIT. This enables us to extract a thermodynamic quantity, the off-diagonal Peltier coefficient α_{xy}, in order to quantitatively explore the quantum criticality. Our main findings are as follows: (1) A sizable Nernst signal is measured on both the superconducting and the insulating sides of the disorder-driven SIT. (2) The Nernst effect amplitude peaks close to the SIT in accordance with recent theoretical predictions. The maximum occurs at $g \simeq 0.35 g_c$. (3) α_{xy} exhibits data collapse over many orders of magnitude, providing a direct determination of the universality class of quantum fluctuations close to the SIT. The scaling analysis is consistent with a clean $(2+1)$D X–Y model yielding critical exponents $\nu \sim 0.7$ and $z \sim 1$.

An InO_x film of thickness 30 nm was e-beam evaporated on MEMpax^{TM} borosilicate glass substrate of thickness 0.4 mm. This substrate was chosen due to its very low thermal conductivity at low temperatures. A Au meander utilized as a heater and two on-chip thermometers (strongly insulating InO_x films) were also evaporated in order to allow a Nernst-effect setup as shown in Fig. 1 (inset). Thermal contact with a 330 mK ^{3}He cryostat was provided at the edge of the substrate farthest from the heater, which determined the direction of the heat current. DC measurements of the transverse thermoelectric voltage and the resistance were carried out with a Keithley 182 digital voltmeter.

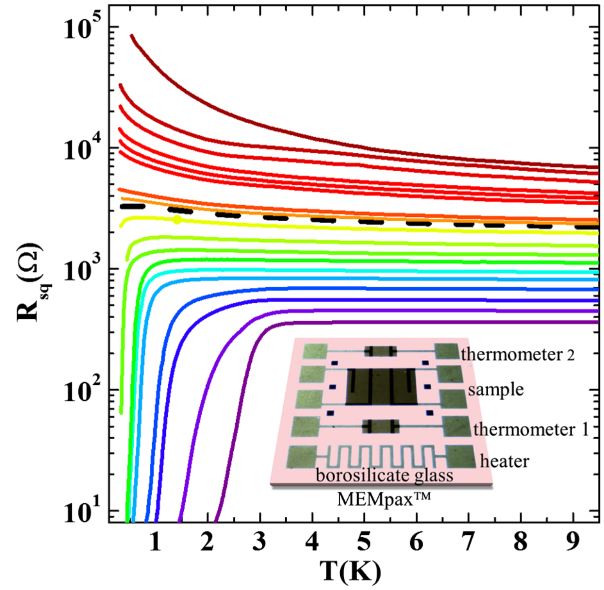

FIG. 1. $R_\square$ versus T for different annealing stages. The quantum phase transition is manifested as the gradual change of ground state from insulator to superconductor as $R_\square$ is lowered. The dashed line is the curve for the film characterized by $g \simeq g_c$, g_c being the value extracted from the scaling analysis below. The curve separates the insulating and superconducting stages. (Inset) Optical image of the chip containing a Au meander as a heater, two strongly insulating films utilized as thermometers, and the InO_x sample. About 1/4 of the chip near thermometer 2 is anchored thermally to the cold head.

The transformation from an insulating ground state to a superconducting one was carried out by increasing the electrical conductance of the sample in stages via low-temperature thermal annealing [65]. An initial highly resistive sample ($R_{\square 5\,K} \simeq 10\ k\Omega$) was created using a high-O_2 partial pressure (8×10^{-5} Torr) during evaporation. It was then taken through several cycles of annealing and measurement, decreasing the room-temperature resistance by ≈5%–10% in each cycle. Resistance versus temperature for the different annealing stages is presented in Fig. 1. The tuning parameter g was chosen to be the sheet resistance $R_\square$ at $T = 5$ K in units of $h/4e^2$. From the data analysis detailed below we find $R^c_{\square 5\,K} = 2410\ \Omega$. This value yields the dashed line in Fig. 1, which separates insulating and superconducting curves. The obtained T_c's for the succeeding stages showed a monotonic increase with decreasing $g = R_{\square 5\,K} \times 4e^2/h$.

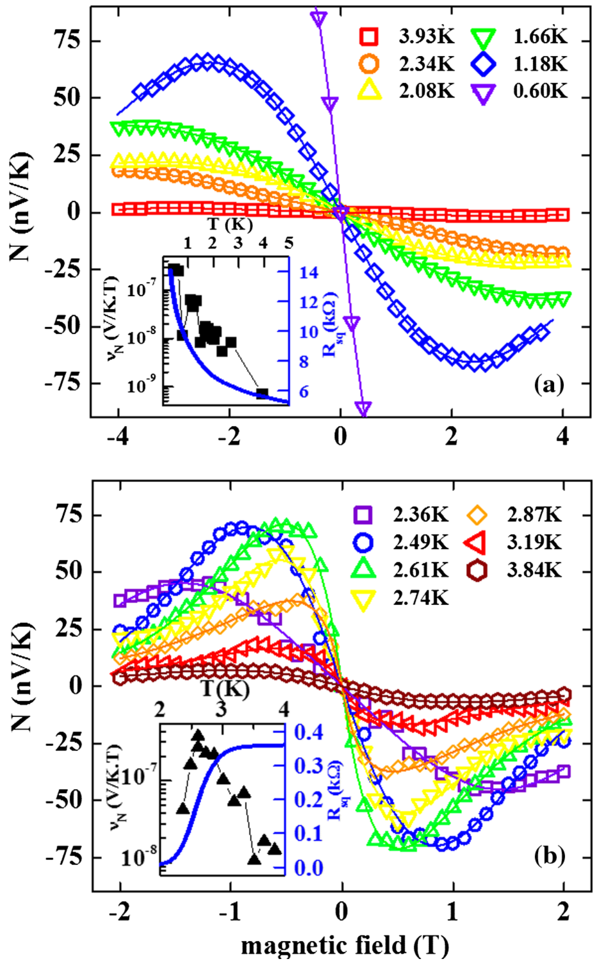

FIG. 2. Nernst signal N versus magnetic field at various temperatures, deep in the (a) insulating ($g/g_c = 2.16$) and (b) superconducting ($g/g_c = 0.15$) sides of the SIT. Also shown are the fitted curves with the *ad hoc* analytic function for extraction of the Nernst coefficient ν_N. (Insets) Extracted Nernst coefficient ν versus T (symbols) and the respective $R_\square(T)$ curves (blue lines).

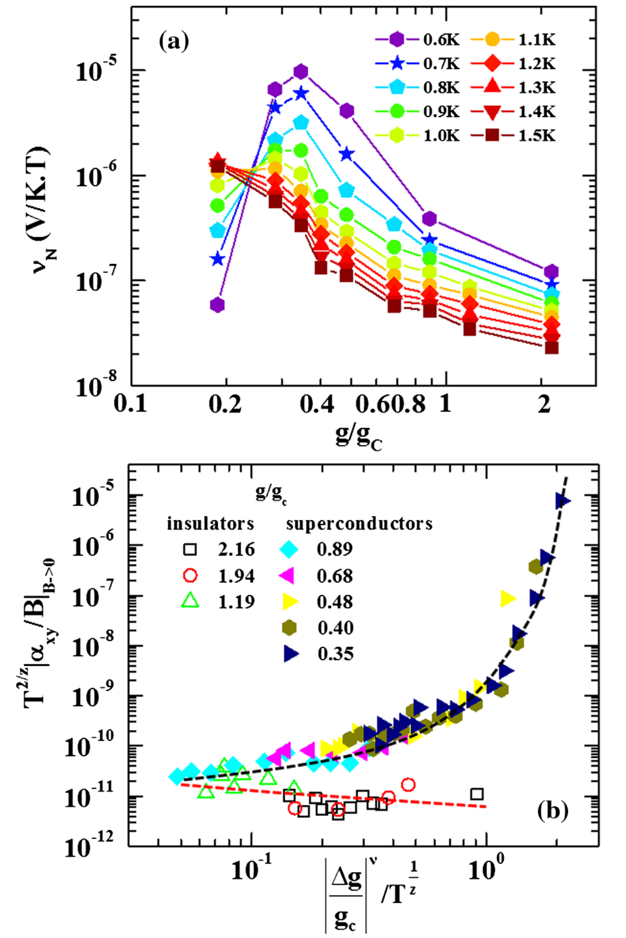

FIG. 3. (a) ν_N versus the normalized quantum tuning parameter, g/g_c showing a peak at $g < g_c$, in agreement with [63]. (b) Scaling plot of the off-diagonal Peltier coefficient α_{xy}. Best data collapse was found for critical exponents $\nu = 0.70$ and $z = 0.99$ and critical resistance $R^c_{\square 5\ \mathrm{K}} = 2410\ \Omega$. $g = R_{\square 5\ \mathrm{K}} \times 4e^2/h$. The dashed lines are guides to the eye.

For each annealing stage, the Nernst signal was measured as a function of magnetic field at different temperatures in the range of 0.4–4 K. In every case, including those in the insulating phase, the field dependence of the signal showed features similar to that of a typical superconductor as reported elsewhere [54]: an asymmetric peak, whose position shifted with temperature. The Nernst coefficient $\nu_N = N/B$ in the limit $B \to 0$ was extracted by fitting the data with an *ad hoc* fitting function $N(B) = \nu_N B e^{-\mu|B|^c}$. Figure 2 depicts such measurements for two annealing stages, one deep in the insulating phase and the other deep in the superconducting phase. It is seen that the overall Nernst features are similar for the two phases, though the temperature dependence is slightly different. For the superconducting stage, ν_N exhibits a peak near the mean field T_c, while for the insulating stage (that obviously does not have a finite T_c), ν_N shows monotonic decrease over several orders of magnitude.

Figure 3(a) shows ν_N as a function of g/g_c through the SIT for different temperatures. At low temperatures, ν_N peaks at $g \simeq 0.35 g_c$. The peak amplitude decreases as the temperature is increased. This is consistent with theoretical predictions [63] and has been attributed to the fact that, in systems with an effective particle-hole symmetry, the Nernst signal can be generally expressed as a product of the resistivity and the transverse Peltier coefficient $N = \rho_{xx}\alpha_{xy}$. The nonmonotonous behavior of ν_N arises from the competition between ρ_{xx}, which increases with g, and α_{xy}, which signifies the strength of the diamagnetic response and hence decreases with g.

We note that ρ_{xx} is a nonequilibrium property signifying the rate of phase slips and is therefore relatively sensitive to microscopic details. In contrast, α_{xy} is approximately proportional to the diamagnetic moment [56,57,59,63,64], i.e., it is a thermodynamic quantity and is expected to be dominated by universal properties. In order to isolate the thermodynamic contribution of the Nernst effect we extract $\alpha_{xy} = N/R_\square$ for each g and T of Fig. 3(a) calculated using the temperature-dependent ρ_{xx}. Since the critical behavior is expected to hold only in the immediate neighborhood of g_c, we focus on samples in the regime $-0.65 < [(\Delta g)/g_c] < 1.2$, since in this regime the analysis described below yielded consistent results (see Supplemental Material [66]). These are plotted in Fig. 3(b) using a scaling ansatz, which assumes proximity to a quantum critical point characterized by critical exponents of Eq. (1). At finite T, universal properties are then expected to depend on g, T via the ratio ξ_τ/L_τ, where $L_\tau \sim 1/T$ is the effective size in the time axis.

To derive the implied scaling form of α_{xy}, we recall the definition

$$\alpha_{xy} = \frac{J_e}{\nabla T}, \tag{2}$$

where the electric current J_e has the physical dimension

$$[J_e] \sim (\text{time})^{-1}(\text{length})^{-(d-1)}. \tag{3}$$

Its dependence on T, B, Δg, and ∇T therefore assumes the general form [67]

$$J_e(T, B, \Delta g, \nabla T) \sim T^{1+(d-1)/z} F_e\left(\frac{B}{T^{2/z}}, \frac{|\nabla T|}{T^{1+1/z}}, \frac{|\Delta g|^\nu}{T^{1/z}}\right), \tag{4}$$

where F_e is a universal scaling function. For small B and ∇T, α_{xy} and hence F_e is linearly dependent on the first two arguments

$$F_e \sim \frac{B}{T^{2/z}} \frac{|\nabla T|}{T^{1+1/z}} f_e\left(\frac{|\Delta g|^\nu}{T^{1/z}}\right), \tag{5}$$

with $f_e(x)$ a single-parameter scaling function. Inserting in Eq. (2), we thus obtain

$$\alpha_{xy} \sim BT^{(d-4)/z} f_e\left(\frac{|\Delta g|^\nu}{T^{1/z}}\right) = \frac{B}{T^{2/z}} f_e\left(\frac{|\Delta g|^{\nu z}}{T}\right), \tag{6}$$

where in the last step we used $d = 2$.

For determining the critical exponents, we fit the experimental values of α_{xy} for different T and g to Eq. (6). The search for the best data collapse was carried out by minimizing the sum of residuals from two “best fitting” polynomial curves, one above and one below g_c, using z, ν, and $R^c_{\square 5\ \mathrm{K}}$ as fitting parameters. The procedure [66] led to $z = 0.99 \pm 0.01$; $\nu = 0.70 \pm 0.09$, and $R^c_{\square 5\ \mathrm{K}} = 2410 \pm 69\ \Omega$. Figure 3(b) shows that this fit yields good data collapse over many orders of magnitude. It is also seen that the scaling form holds on both sides of the QPT, with different forms of the scaling function f_e. This result is consistent with a clean $(2+1)$D X–Y model, where particle-hole symmetry is effectively obeyed. It provides confirmation that the SIT is a quantum phase transition driven by interaction-dominated quantum fluctuations of the superconducting order parameter in 2D.

The X–Y model is in agreement with the so-called bosonic model for the SIT [32] in which the system can be modeled by an array of sites, each one characterized by a local superconducting order parameter amplitude and phase and the probability to obtain phase coherence, and hence global superconductivity, depends on the ratio E_C/E_J. InO films, despite being morphologically uniform, have been shown to include “emergent granularity” in the form of superconducting puddles embedded in an insulating matrix [68–75]. Hence, local superconductivity can be present in the insulating phase as well. The bosonic model separates between the mean-field critical temperature T_c^{MF}, which sets the Cooper-pair breaking scale, and T_{BKT}, which is related to the proliferation of free vortices whose motion is measured by transport. The finite Nernst effect we observe on the insulator indicates the presence of vortex motion in this phase as well, thus providing further confirmation for the relevance of the X–Y model to our systems. In this context, we note a few earlier observations on InO_x, which revealed the presence of superconductivity in the insulator. The role of vortexlike superconducting fluctuations in the insulating phase were demonstrated by measurements of the “vortex ratchet effect” [27] and of Little-Parks oscillations [76] on both sides of the SIT. In addition, tunneling density of states experiments detected the presence of a superconducting energy gap, and thereby Cooper pairing, not only above T_c [26], but also on the insulating side of the disorder-driven SIT [77]. These fluctuations of the phase and amplitude of the order parameter were picked up by our Nernst measurements. Our results indicate that the true critical behavior (which takes over in the limit of long length scales) is not sensitive to disorder, but rather dominated by a coarse-grained effective model of coupled superconducting puddles.

We are grateful to I. Volotsenko for technical help and to K. Behnia for useful discussions. This research was supported by the Israel Science Foundation, Grants No. 783/17 (A. F.) and No. 231/14 (E. S.).

[1] S. Sachdev, *Quantum Phase Transitions* (Cambridge University Press, Cambridge, England, 2001).
[2] M. Strongin, R. S. Thompson, O. F. Kammerer, and J. E. Crow, Phys. Rev. B **1**, 1078 (1970).
[3] R. C. Dynes, A. E. White, J. M. Graybeal, and J. P. Garno, Phys. Rev. Lett. **57**, 2195 (1986).
[4] D. B. Haviland, Y. Liu, and A. M. Goldman, Phys. Rev. Lett. **62**, 2180 (1989).
[5] J. M. Valles, R. C. Dynes, and J. P. Garno, Phys. Rev. Lett. **69**, 3567 (1992).
[6] A. Frydman, O. Naaman, and R. C. Dynes, Phys. Rev. B **66**, 052509 (2002).

[7] N. Hadacek, M. Sanquer, and J.-C. Villégier, Phys. Rev. B **69**, 024505 (2004).

[8] M. D. Stewart, A. Yin, J. M. Xu, and J. M. Valles, Science **318**, 1273 (2007).

[9] B. Sacépé, C. Chapelier, T. I. Baturina, V. M. Vinokur, M. R. Baklanov, and M. Sanquer, Phys. Rev. Lett. **101**, 157006 (2008).

[10] S. M. Hollen, H. Q. Nguyen, E. Rudisaile, M. D. Stewart, J. Shainline, J. M. Xu, and J. M. Valles, Phys. Rev. B **84**, 064528 (2011).

[11] S. V. Postolova, A. Y. Mironov, M. R. Baklanov, V. M. Vinokur, and T. I. Baturina, Sci. Rep. **7**, 1718 (2017).

[12] T. I. Baturina, V. M. Vinokur, A. Y. Mironov, N. M. Chtchelkatchev, D. A. Nasimov, and A. V. Latyshev, Europhys. Lett. **93**, 47002 (2011).

[13] S. Poran, T. Nguyen-Duc, A. Auerbach, N. Dupuis, A. Frydman, and O. Bourgeois, Nat. Commun. **8**, 14464 (2017).

[14] M. A. Paalanen, A. F. Hebard, and R. R. Ruel, Phys. Rev. Lett. **69**, 1604 (1992).

[15] A. Yazdani and A. Kapitulnik, Phys. Rev. Lett. **74**, 3037 (1995).

[16] V. F. Gantmakher, M. V. Golubkov, V. T. Dolgopolov, G. E. Tsydynzhapov, and A. A. Shashkin, J. Exp. Theor. Phys. Lett. **68**, 363 (1998).

[17] G. Sambandamurthy, L. W. Engel, A. Johansson, and D. Shahar, Phys. Rev. Lett. **92**, 107005 (2004).

[18] G. Sambandamurthy, L. W. Engel, A. Johansson, E. Peled, and D. Shahar, Phys. Rev. Lett. **94**, 017003 (2005).

[19] M. A. Steiner, G. Boebinger, and A. Kapitulnik, Phys. Rev. Lett. **94**, 107008 (2005).

[20] T. I. Baturina, J. Bentner, C. Strunk, M. R. Baklanov, and A. Satta, Physica (Amsterdam) **359B–361B**, 500 (2005).

[21] T. I. Baturina, C. Strunk, M. R. Baklanov, and A. Satta, Phys. Rev. Lett. **98**, 127003 (2007).

[22] R. W. Crane, N. P. Armitage, A. Johansson, G. Sambandamurthy, D. Shahar, and G. Grüner, Phys. Rev. B **75**, 094506 (2007).

[23] V. M. Vinokur, T. I. Baturina, M. V. Fistul, A. Y. Mironov, M. R. Baklanov, and C. Strunk, Nature (London) **452**, 613 (2008).

[24] R. Ganguly, I. Roy, A. Banerjee, H. Singh, A. Ghosal, and P. Raychaudhuri, Phys. Rev. B **96**, 054509 (2017).

[25] D. Shahar and Z. Ovadyahu, Phys. Rev. B **46**, 10917 (1992).

[26] B. Sacépé, T. Dubouchet, C. Chapelier, M. Sanquer, M. Ovadia, D. Shahar, M. Feigel'man, and L. Ioffe, Nat. Phys. **7**, 239 (2011).

[27] S. Poran, E. Shimshoni, and A. Frydman, Phys. Rev. B **84**, 014529 (2011).

[28] M. Mondal, A. Kamlapure, M. Chand, G. Saraswat, S. Kumar, J. Jesudasan, L. Benfatto, V. Tripathi, and P. Raychaudhuri, Phys. Rev. Lett. **106**, 047001 (2011).

[29] K. A. Parendo, K. H. S. B. Tan, A. Bhattacharya, M. Eblen-Zayas, N. E. Staley, and A. M. Goldman, Phys. Rev. Lett. **94**, 197004 (2005).

[30] A. D. Caviglia, S. Gariglio, N. Reyren, D. Jaccard, T. Schneider, M. Gabay, S. Thiel, G. Hammerl, J. Mannhart, and J.-M. Triscone, Nature (London) **456**, 624 (2008).

[31] A. T. Bollinger, G. Dubuis, J. Yoon, D. Pavuna, J. Misewich, and I. Božović, Nature (London) **472**, 458 (2011).

[32] M. P. A. Fisher, Phys. Rev. Lett. **65**, 923 (1990).

[33] M. P. A. Fisher, P. B. Weichman, G. Grinstein, and D. S. Fisher, Phys. Rev. B **40**, 546 (1989).

[34] S. L. Sondhi, S. M. Girvin, J. P. Carini, and D. Shahar, Rev. Mod. Phys. **69**, 315 (1997).

[35] Y. H. Li and S. Teitel, Phys. Rev. B **40**, 9122 (1989).

[36] M. Campostrini, M. Hasenbusch, A. Pelissetto, P. Rossi, and E. Vicari, Phys. Rev. B **63**, 214503 (2001).

[37] M. P. A. Fisher, G. Grinstein, and S. M. Girvin, Phys. Rev. Lett. **64**, 587 (1990).

[38] E. S. Sørensen, M. Wallin, S. M. Girvin, and A. P. Young, Phys. Rev. Lett. **69**, 828 (1992).

[39] M. C. Cha and S. M. Girvin, Phys. Rev. B **49**, 9794 (1994).

[40] N. Prokof'ev and B. Svistunov, Phys. Rev. Lett. **92**, 015703 (2004).

[41] S. Iyer, D. Pekker, and G. Refael, Phys. Rev. B **85**, 094202 (2012).

[42] T. Vojta, J. Crewse, M. Puschmann, D. Arovas, and Y. Kiselev, Phys. Rev. B **94**, 134501 (2016).

[43] A. F. Hebard and M. A. Paalanen, Phys. Rev. Lett. **65**, 927 (1990).

[44] M. H. Theunissen and P. H. Kes, Phys. Rev. B **55**, 15183 (1997).

[45] N. Markovic, C. Christiansen, and A. M. Goldman, Phys. Rev. Lett. **81**, 5217 (1998).

[46] N. Marković, C. Christiansen, A. M. Mack, W. H. Huber, and A. M. Goldman, Phys. Rev. B **60**, 4320 (1999).

[47] V. F. Gantmakher, M. V. Golubkov, V. T. Dolgopolov, A. A. Shashkin, and G. E. Tsydynzhapov, JETP Lett. **71**, 473 (2000).

[48] E. Bielejec and W. Wu, Phys. Rev. Lett. **88**, 206802 (2002).

[49] H. Aubin, C. A. Marrache-Kikuchi, A. Pourret, K. Behnia, L. Bergé, L. Dumoulin, and J. Lesueur, Phys. Rev. B **73**, 094521 (2006).

[50] X. Shi, P. V. Lin, T. Sasagawa, V. Dobrosavljević, and D. Popović, Nat. Phys. **10**, 437 (2014).

[51] S. Park, J. Shin, and E. Kim, Sci. Rep. **7**, 42969 (2017).

[52] C. A. Marrache-Kikuchi, H. Aubin, A. Pourret, K. Behnia, J. Lesueur, L. Bergé, and L. Dumoulin, Phys. Rev. B **78**, 144520 (2008).

[53] K. Behnia, J. Phys. Condens. Matter **21**, 113101 (2009).

[54] K. Behnia and H. Aubin, Rep. Prog. Phys. **79**, 046502 (2016).

[55] I. Ussishkin, S. L. Sondhi, and D. A. Huse, Phys. Rev. Lett. **89**, 287001 (2002).

[56] D. Podolsky, S. Raghu, and A. Vishwanath, Phys. Rev. Lett. **99**, 117004 (2007).

[57] S. A. Hartnoll, P. K. Kovtun, M. Müller, and S. Sachdev, Phys. Rev. B **76**, 144502 (2007).

[58] K. Michaeli and A. M. Finkel'stein, Europhys. Lett. **86**, 27007 (2009).

[59] G. Wachtel and D. Orgad, Phys. Rev. B **90**, 184505 (2014).

[60] Y. Wang, L. Li, and N. P. Ong, Phys. Rev. B **73**, 024510 (2006).

[61] A. Pourret, H. Aubin, J. Lesueur, C. A. Marrache-Kikuchi, L. Bergé, L. Dumoulin, and K. Behnia, Phys. Rev. B **76**, 214504 (2007).

[62] P. Spathis, H. Aubin, A. Pourret, and K. Behnia, Europhys. Lett. **83**, 57005 (2008).

[63] Y. Atzmon and E. Shimshoni, Phys. Rev. B **87**, 054510 (2013).

[64] Y. Schattner, V. Oganesyan, and D. Orgad, Phys. Rev. B **94**, 235130 (2016).
[65] Z. Ovadyahu, J. Phys. C **19**, 5187 (1986).
[66] See Supplemental Material at http://link.aps.org/supplemental/10.1103/PhysRevLett.121.047003 for brief description.
[67] M. J. Bhaseen, A. G. Green, and S. L. Sondhi, Phys. Rev. B **79**, 094502 (2009).
[68] D. Kowal and Z. Ovadyahu, Solid State Commun. **90**, 783 (1994).
[69] D. Kowal and Z. Ovadyahu, Physica (Amsterdam) **468C**, 322 (2008).
[70] E. Shimshoni, A. Auerbach, and A. Kapitulnik, Phys. Rev. Lett. **80**, 3352 (1998).
[71] Y. Dubi, Y. Meir, and Y. Avishai, Nature (London) **449**, 876 (2007).
[72] Y. Imry, M. Strongin, and C. Homes, Physica (Amsterdam) **468C**, 288 (2008).
[73] N. Trivedi, R. T. Scalettar, and M. Randeria, Phys. Rev. B **54**, R3756 (1996).
[74] A. Ghosal, M. Randeria, and N. Trivedi, Phys. Rev. B **65**, 014501 (2001).
[75] K. Bouadim, Y. L. Loh, M. Randeria, and N. Trivedi, Nat. Phys. **7**, 884 (2011).
[76] G. Kopnov, O. Cohen, M. Ovadia, K. H. Lee, C. C. Wong, and D. Shahar, Phys. Rev. Lett. **109**, 167002 (2012).
[77] D. Sherman, G. Kopnov, D. Shahar, and A. Frydman, Phys. Rev. Lett. **108**, 177006 (2012).